Bulgarian Chemical Communications, Volume 50, Special issue H (pp. 201–208) 2018

A DFT study of ammonia dissociation over Mo_3N_2 cluster

S. F. Zaman

Chemical and Materials Engineering Department, Faculty of Engineering, King Abdulaziz University, P.O. Box 80204, Jeddah 21589, Saudi Arabia

Received: February 05, 2018; Revised: March 04, 2018

Density functional theory (DFT) calculations were performed to generate the potential energy surface of ammonia decomposition over a Mo_3N_2 cluster by investigating elementary surface reaction steps of the dehydrogenation pathway of NH_3. Ontop adsorption of NHx (x = 0–3) species over an Mo atom was found to be the most favourable adsorption arrangement. The rate limiting step for NH_3 dissociation was the abstraction of the 2nd hydrogen according to the following surface elementary reaction (NH_2*ad → NH*ad + H*ad) with an activation energy of 41.2 kcal/mol and an endothermic heat of reaction of 28.05 kcal/mol. The Nitrogen dissociation energy 35.19 kcal/mol over the cluster is much higher than over the Ru(0001) surface.

Key words: DFT, NH_3 dissociation, Mo_3N_2 cluster, adsorption energy, potential energy surface.

INTRODUCTION

Hydrogen is the ideal fuel that can mitigate environmental problems connected with energy production, since the water is the only combustion product. The use of clean hydrogen containing low (< 10 ppm) concentration of CO as a fuel in proton exchange membrane fuel cells (PEMFC) is a very effective way to produce eclectic energy with efficiency up to 60% [1–3]. The fuel cell generators are noiseless devices, which have no harmful emissions generation. The main obstacle for practical application of hydrogen as a fuel for on board devices is the very low energy capacity per unit hydrogen gas volume. Therefore, the hydrogen storage is a problem of crucial importance for the future practical use of hydrogen in on board devices. One of the possible ways to overcome this negative circumstance is the production of clean hydrogen by NH_3 decomposition in on board catalytic reactors. NH_3 molecule is the richest for hydrogen molecule. It contains 17.8 wt.% hydrogen. This means that at 20 °C and 8.6 bar from one m^3 liquid NH_3 108 kg H_2 can be produced [4]. The use of liquid NH_3 as a hydrogen storage also offers a number of technological advantages. Because of the fact that obtained hydrogen does not contain any traces of CO. Thus the use of NH_3 for on board preparation of clean hydrogen is very promising technology. Thermodynamic data shows that at atmospheric pressure and 400 °C the possible achievable degree of conversion of NH_3 is 99.0%. However, in the catalytic experiments with different types of catalysts obtained degrees of conversion are lower at much higher temperatures.

Supported Ru is the most active catalyst [5], but Ru scarce availability in nature and very high price make it not suitable for wide applications. The decomposition catalysts have different chemical nature i.e. metals from Group VIII (Fe, [6–9] Co, Ni [10–13], Ru [13–20] or supported on oxides or on MWCNTs, metal carbides and nitrides like MoNx, VCx, MoCx, VNx, etc. Therefore, it is of great importance to receive information about some of the elementary steps of the mechanism of this reaction. NH_3 decomposition is a reversible endothermic reaction given by the following equation:

$$NH_3 = 0.5\ N_2 + 1.5\ H_2 \quad [\Delta Hr = +46\ kJ/mol]$$

Recently, the reaction of NH_3 decomposition has attracted much attention. Several studies have been reported results from ammonia dissociation studies on different catalyst surfaces using DFT approach [22–28]. Interestingly, no DFT work is reported for Mo_2N based catalysts.

This paper presents the results of DFT study of the ammonia dissociation mechanism on a simple Mo_3N_2 cluster. This cluster was selected for two reasons. (i) The Mo_3N_2 cluster can be used as a simple model of the Mo_2N catalyst surface. Therefore, by the studying Mo_3N_2 cluster we can obtain reliable information about surface reaction steps and we will be able to determine the potential energy surface (PES) for this dissociation reaction. (ii) The use Mo_3N_2 cluster leads to substantial reduction of the computational cost.

* To whom all correspondence should be sent
E-mail: zfsharif@gmail.com; sfzaman@kau.edu.sa

CALCULATION PROCEDURE

The DMol3 module of Material Studio (version 7.0) from Accelrys Inc. (San Diego, CA, USA) was used to perform the DFT calculations. Accordingly, the electronic wave functions are expanded in numerical atomic basis sets defined on an atomic-centered spherical polar mesh. The double-numerical plus P-function (DNP) of all electron basis set, was used for all the calculations. The DNP basis set includes one numerical function for each occupied atomic orbital and a second set of functions for valence atomic orbitals, plus a polarization p-function on all atoms. Each basis function was restricted to a cutoff radius of 4.9 Å, allowing for efficient calculations without loss of accuracy. The Kohn-Sham equations [29] were solved by a self-consistent field procedure using PW91 functional with GGA for exchange correlation [30-32]. The techniques of direct inversion in an iterative subspace with a size value of six and thermal smearing of 0.005 Ha were applied to accelerate convergence. The optimization convergence thresholds for energy change, maximum force and maximum displacement between the optimization cycles were 0.00001 Ha, 0.002 Ha/Å and 0.005 Å, respectively. The k-point set of (1x1x1) was used for all calculations. The activation energy of interaction between two surface species was identified by complete linear synchronous transit and quadratic synchronous transit search methods [33] followed by TS confirmation through the nudge elastic band method [34]. Spin polarization was imposed in all the calculations. The adsorption energy of an element (i.e. molecule or atom) was found according to the following formula:

$$E_{ad} = 1/n\,[E_{slab+element} - \{E_{empty\ slab} + E_{element}\}],$$

where n is the number of adsorbed species.

Mo_3N_2 CLUSTER FORMATION

The Mo_3N_2 cluster, comprising of five atoms, is depicted in Fig. 1, where Mo atoms are indexed as $Mo_{(1)}$, $Mo_{(2)}$ and $Mo_{(3)}$ and nitrogen atoms as $N_{(4)}$ and $N_{(5)}$. The cluster structure was optimized using geometric optimization imposing no constraints on atomic position. After geometric optimization the cluster atomic position was fixed to investigate NH_3 decomposition. The optimised distance between $Mo_{(1)}$–$Mo_{(2)}$ is 2.236 Å, $Mo_{(1)}$–$Mo_{(3)}$ is 2.753 Å, $Mo_{(2)}$–$Mo_{(3)}$ is 2.842 Å, $Mo_{(1)}$–$N_{(4)}$ is 2.042 Å, and $Mo_{(1)}$–$N_{(5)}$ is 2.042 Å. The angle, ∠ $Mo_{(1)}$–$N_{(4)}$–$Mo_{(2)}$ is 66.95°, ∠ $Mo_{(1)}$–$N_{(4)}$–$Mo_{(3)}$ is 88.36°, ∠ $Mo_{(2)}$–$N_{(4)}$–$Mo_{(3)}$ is 92.26°, ∠ $Mo_{(1)}$–$N_{(4)}$–$Mo_{(2)}$ is 66.57°, ∠ $Mo_{(1)}$–$N_{(4)}$–$Mo_{(3)}$ is 88.37°, ∠ $Mo_{(2)}$–$N_{(5)}$–$Mo_{(3)}$ is 92.28°. The reaction sequence investigated on Mo_3N_2 cluster is as follows:

$$NH_3{*}ad \rightarrow NH_2{*}ad + H{*}ad \quad (1)$$

$$NH{*}ad \rightarrow NH{*}ad + H{*}ad \quad (2)$$

$$NH{*}ad \rightarrow N{*}ad + H{*}ad \quad (3)$$

Also the nitrogen molecule decomposition over the cluster was investigated

$$N_2{*}ad \rightarrow N{*}ad + N{*}ad. \quad (4)$$

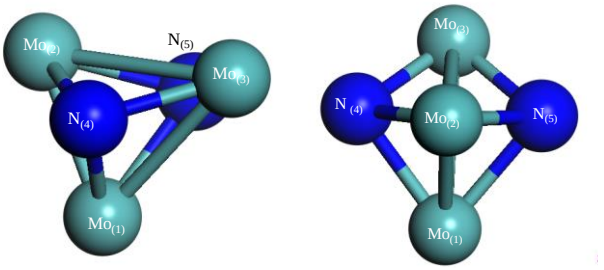

Fig. 1. The optimized Mo_3N_2 cluster structure with atom indexing.

AMMONIA (NH_3) ADSORPTION ON THE CLUSTER

Ammonia molecule was placed on the three different Mo atoms of the cluster (indexed as 1, 2, 3) to seek the preferred adsorption position or the minimum energy configuration (Fig. 2). It was found that NH_3 was absorbed on-top position over Mo atom. The adsorption energy on different Mo atoms indexing (1), (2) and (3) was −25.35 kcal/mol, −21.49 kcal/mol, and −20.48 kcal/mol, and the bond length between $Mo_{(x)}$ and N atom (of NH_3) was 2.33 Å, 2.34 Å and 2.36 Å, respectively. $Mo_{(1)}$ atom is the preferred adsorption location for the NH_3 molecule. The adsorption arrangements are shown in Fig. 2. Researchers previously reported the value of NH_3 adsorption energy on Ni (110) surface of 20.75 kcal/mol [35], 17.29 kcal/mol on Ni (111) surface [36], 15.78 kcal/mol on Co (111) surface [36] and on an Fe cluster 8.83 kcal/mol [37]. So NH_3 is more strongly adsorbed on the Mo_3N_2 cluster compared to other potential NH_3 decomposition catalyst surfaces. Table 1 shows the charge distribution on the cluster atoms and on the N atom of NH_x (x = 1–3) species prior to and after being adsorbed on the cluster. After adsorbing NH_3 on the cluster at the $Mo_{(1)}$ atom there was a decrease in positive charge on $Mo_{(1, 2, 3)}$ atom of the cluster, and the negative charge on the $N_{(4)}$ and $N_{(5)}$ atoms decreased compared to the empty cluster. The negative charge on the N atom of NH_3 increased upon adsorption. Clearly electron transferred from the $N_{(5)}$ and $N_{(4)}$ atoms (of the cluster) to the nitrogen atom (NH_3 species) and Mo

atoms of the cluster during the surface bond formation.

FIRST HYDROGEN ATOM ABSTRACTION FROM AMMONIA

The abstraction of the 1st hydrogen (Fig. 2) was investigated according to the elementary surface reaction NH_3*ad → NH_2*ad + H*ad. NH_3 adsorbed on $Mo_{(1)}$ atom was taken as the reactant configuration as it has the lowest energy configuration. The NH_2 species was adsorbed on $Mo_{(1)}$ atom. Preferred hydrogen co-adsorption location was investigated on $Mo_{(2)}$ and $Mo_{(3)}$ and $N_{(4)}$ atom. The [NH_2*ad + H*ad] configuration had the lowest energy configuration when NH_2 species was adsorbed on $Mo_{(1)}$ and the H atom adsorbed on $Mo_{(3)}$, with an adsorption energy of −77.70 kcal/mol. The distance between $Mo_{(1)}$ and N of NH_2 species is 2.007 Å and $Mo_{(3)}$ and H is 1.791 Å. A very similar adsorption energy, −77.41 kcal/mol, was found when the H atom was adsorbed on $Mo_{(2)}$. The distance between $Mo_{(1)}$ and N of NH_2 species is 2.07 Å and $Mo_{(2)}$ and the H is 1.787 Å. The H atom is adsorbed on $N_{(4)}$ atom showed the largest adsorption energy among the three arrangements, −70.99 kcal/mol, and is least favourable. The transition state search was performed for the first two arrangements. Fig. 2 shows the adsorption configuration and adsorption energies and atomic distances.

The activation barrier for the product arrangement NH_2 on $Mo_{(1)}$ and H on $Mo_{(3)}$ was found to be 18.41 kcal/mol with an exothermic heat of reaction of −16.47 kcal/mol. The activation barrier for the product arrangement NH_2 on $Mo_{(1)}$ and H on $Mo_{(2)}$ was found to be 18.19 kcal/mol with an exothermic heat of reaction of −15.88 kcal/mol. The energy difference is very small but for the 2nd arrangement where the H atom is adsorbed on $Mo_{(2)}$, less activation energy is required. Hence it is a much more favourable dissociation path for the 1st H abstraction. The activation barrier of the 1st hydrogen abstraction on Ni (110) surface it is 22.14 kcal/mol [35], on Co (111) surface it is 23.29 kcal/mol [36], on an Fe cluster it is 34.13 kcal/mol [37] and on Pt (111) surface 26.76 kcal/mol [38]. The Mo_3N_2 cluster is more reactive towards first hydrogen abstraction compared to other active catalysts for ammonia dissociation, which is an important characteristic of the Mo_3N_2 cluster.

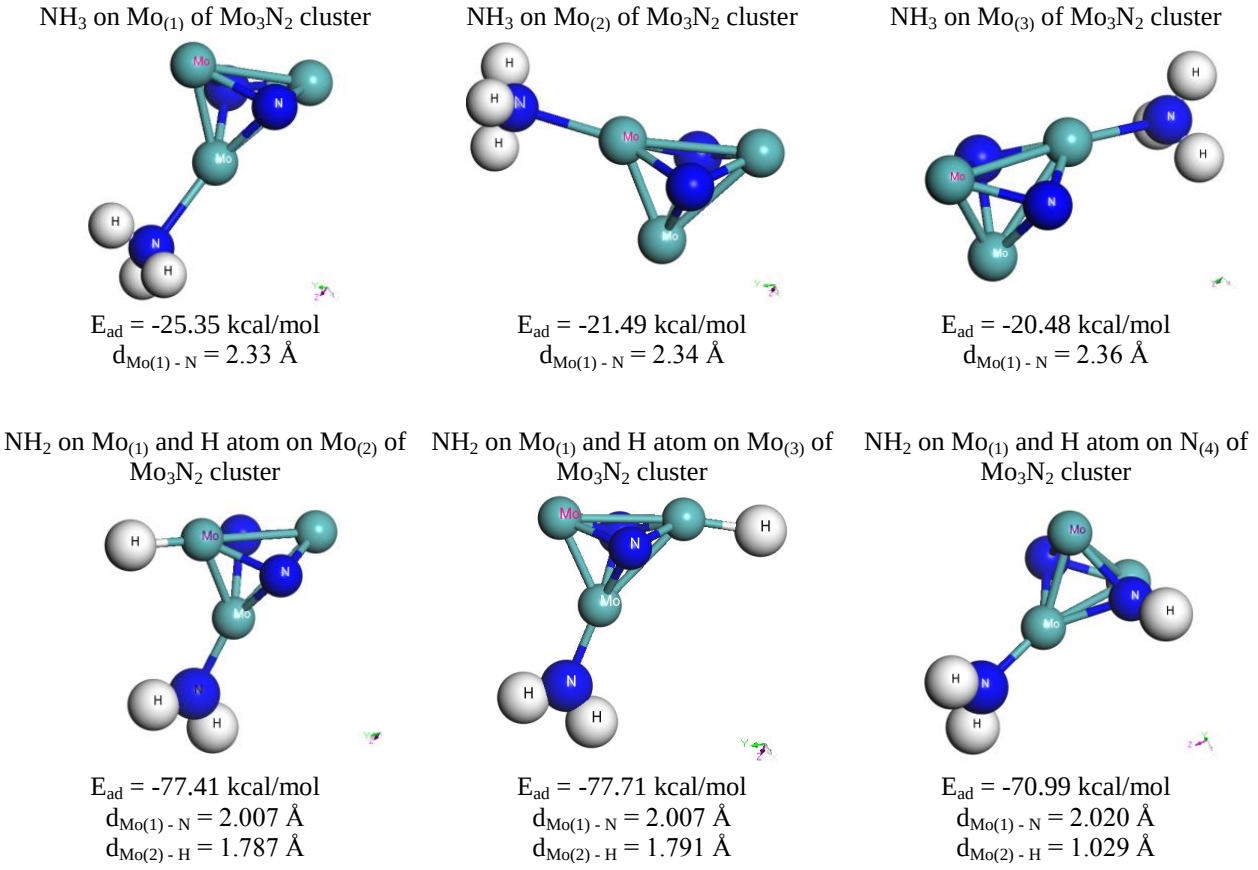

Fig. 2. Reactant and product configuration, adsorption energies and atomic distance for 1st hydrogen abstraction from NH_3 over Mo_3N_2.

NH_2 ADSORPTION ENERGY

The NH_2 species was strongly adsorbed ontop of the $Mo_{(1)}$ atom of Mo_3N_2 cluster (Fig. 3), compared to NH_3 molecule, with an adsorption energy of −92.33 kcal/mol. The distance between $Mo_{(1)}$ and N (NH_2 species) is 2.022 Å. A bridge adsorption mode of NH_2, where the N atom (of NH_2 species) was bound to $Mo_{(1)}$ and $Mo_{(2)}$ has adsorption energy of −80.11 kcal/mol, which is much less than on-top adsorption mode. NH_2 species prefer a bridge position having an adsorption energy of −73.33 kcal/mol on Ni (110) surface [35], on Fe(110) surface adsorption energy is −73.10 kcal/mol [38], on Co (111) surface adsorption energy is −63.78 kcal/mol [36] and on Ni (111) surface adsorption energy is −62.95 kcal/mol [36]. NH_2 species is more strongly bound to the Mo_3N_2 surface. The charge distribution over the cluster atoms and NH_2 species are reported in Table 1. There is an increase in positive charge over the Mo atoms suggesting electron transfer from the Mo atoms of the cluster for the surface bond formation which is confirmed by the increase in negative charge on the N atom (of NH_2 species). The charge on the cluster N atoms undergoes a small increase in negative charge compared to the empty cluster.

Table 1. Mulliken atomic charge over the atoms in the Mo_3N_2 cluster and the adsorbed species during ammonia decomposition.

Atom (index) in the cluster and adsorbed species	Empty Cluster [e]	Adsorbed NH_3 on $Mo_{(1)}$ [e]	Adsorbed NH_2 on $Mo_{(1)}$ [e]	Adsorbed NH on $Mo_{(1)}$ [e]
Mo (1)	0.585	0.447	0.783	0.858
Mo (2)	0.420	0.355	0.442	0.486
Mo (3)	0.585	0.528	0.656	0.655
N (4)	-0.711	-0.717	-0.729	-0.728
N (5)	-0.711	-0.571	-0.730	-0.728
N (Adsorbed NH_x species on Cluster)	-	-0.571	-0.786	-0.701
N (Free NH_x Species)	-	-0.430	-0.331	-0.167

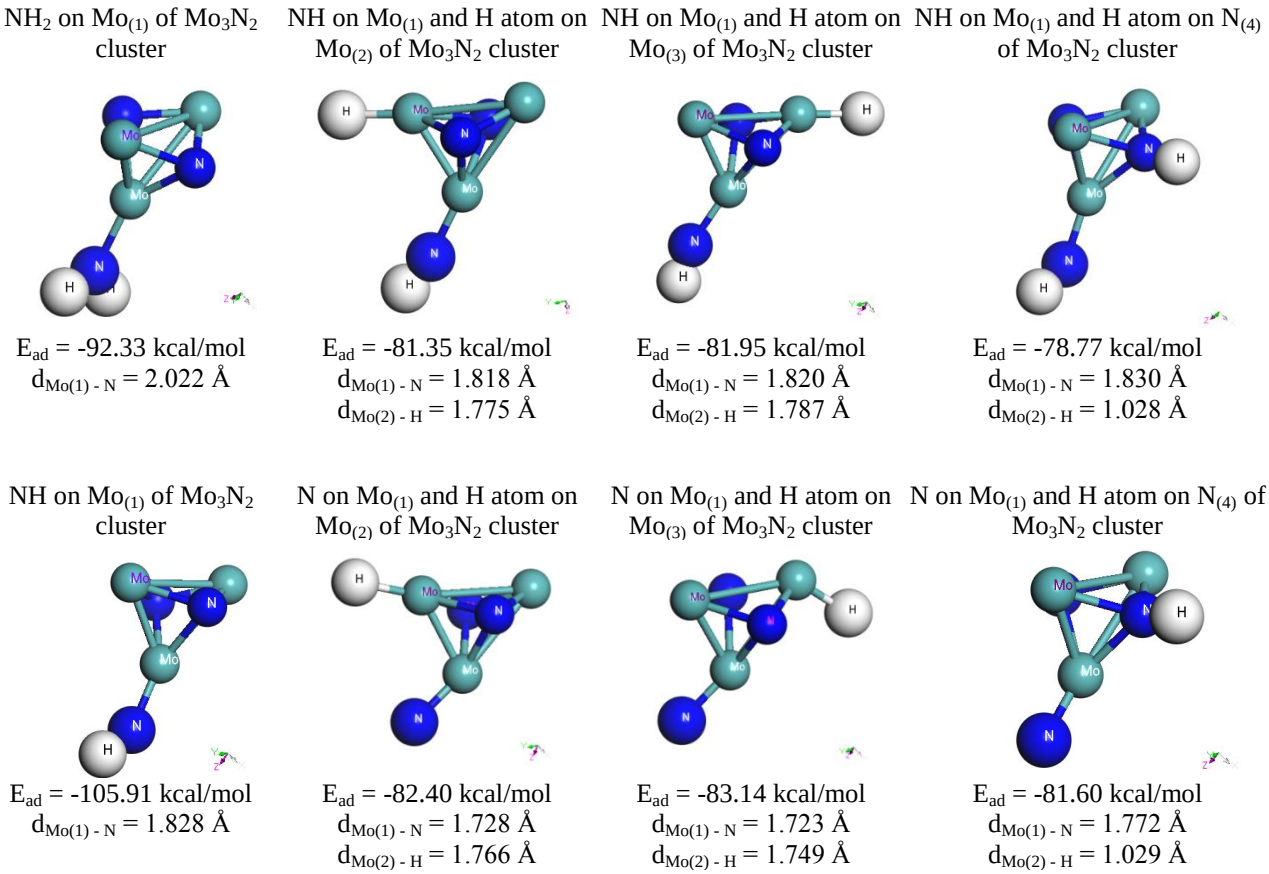

Fig. 3. Reactant and product configuration, adsorption energies and atomic distance for 2nd and 3rd hydrogen abstraction fromNH_3 over Mo_3N_2.

SECOND HYDROGEN ATOM ABSTRACTION

The abstraction of the 2nd hydrogen was investigated according to the elementary surface reaction NH_2*ad → NH*ad + H*ad. NH* species adsorbed on the $Mo_{(1)}$ atom was taken as the reactant configuration (Fig. 3). For the product configuration, three different surface arrangement were investigated with NH species on $Mo_{(1)}$ and H on three different positions, $Mo_{(2)}$, $Mo_{(3)}$ and $N_{(4)}$ atom. The binding energies are −95.98 kcal/mol, 81.95 kcal/mol and −78.78 kcal/mol, respectively. Hence NH species on $Mo_{(1)}$ and H atom on $Mo_{(2)}$ is energetically the most favourable product configuration where the atomic distance between $Mo_{(1)}$ and N (NH species) is 1.818 Å and between $Mo_{(2)}$ and H atom is 1.775 Å. Fig. 3 shows the adsorption configuration and adsorption energies and atomic distances. A transition state search found that the dissociation energy barrier is 41.20 kcal/mol with an endothermic reaction energy of 28.08 kcal/mol. X. Duan *et al.* [35] reported an activation barrier of 37.59 kcal/mol over Ni(110) plane, over Pt (111) surface the barrier is 36.09 kcal/mol [38], over Co (111) surface the barrier is 4.84 kcal/mol [36] and over Fe cluster the barrier 20.75 kcal/mol [37].

NH ADSORPTION ENERGY

The NH species is strongly adsorbed ontop of the $Mo_{(1)}$ atom of the Mo_3N_2 cluster (Fig. 3) compared to NH_3 and NH_2, with an adsorption energy of -105.91 kcal/mol. The distance between $Mo_{(1)}$ and N (NH species) is 1.828 Å. A bridge adsorption mode of NH, where the N atom is bound to $Mo_{(1)}$ and $Mo_{(2)}$, has an adsorption energy of -94.79 kcal/mol, which is much less than the on-top adsorption mode. The NH species prefer a bridge position having an adsorption energy of −91.08 kcal/mol on Ni(110) [35], on Co(111) surface, the hcp location has adsorption energy of -106.76 kcal/mol [36] and on Ni(111) surface, the fcc location has adsorption energy of −105.38 kcal/mol [36]. There is an increase in positive charge over the cluster Mo atoms, especially on the $Mo_{(1)}$ and $Mo_{(3)}$ suggesting the electron transfer from the Mo atoms of the cluster for the surface bond formation with NH species, which is confirmed by the increase in negative charge on the N atom (of NH species). The charge on the cluster N atoms undergoes small increase in negative charge.

THIRD HYDROGEN ATOM ABSTRACTION

The abstraction of the 3rd hydrogen atom from NH_3 was investigated according to the elementary surface reaction NH*ad → N*ad + H*ad (Fig. 3). The NH species adsorbed on the $Mo_{(1)}$ atom was taken as the reactant configuration. For the product configuration three different surface arrangements were investigated with N species on $Mo_{(1)}$ and H on three different positions, $Mo_{(2)}$, $Mo_{(3)}$ and $N_{(4)}$ atom with binding energy −82.40 kcal/mol, −83.14 kcal/mol and −77.41 kcal/mol, respectively. Hence the N species on $Mo_{(1)}$ and the H atom on $Mo_{(3)}$ is energetically the most favourable product configuration where the atomic distance between $Mo_{(1)}$ and N (NH species) is 1.723 Å and $Mo_{(2)}$ and H is 1.749 Å. Fig. 3 shows the adsorption configuration, adsorption energies and atomic distances. A transition state search found that the dissociation energy barrier is 33.89 kcal/mol with the endothermic reaction energy of 28.38 kcal/mol. Duan X. *et al.* [35] reported an activation barrier 20.52 kcal/mol over Ni(110) plane, over Pt(111) surface the barrier is 34.42 kcal/mol [38], over Co(111) surface the barrier is 24.44 kcal/mol [36] and over Fe cluster 7.84 kcal/mol [37]. Charges on atoms of the cluster and on the adsorbed molecules are tabulated in Table 1.

POTENTIAL ENERGY SURFACE OF NH_3 DISSOCIATION

The activation barrier and reaction energies of the surface elementary reactions of ammonia decomposition for the Mo_3N_2 cluster and some other potential surfaces are tabulated in Table 2 and the potential energy surface on the Mo_3N_2 cluster is depicted in Fig. 4, taking free Mo_3N_2 cluster and free NH_3 molecule as the zero energy reference. Only the 1st hydrogen abstraction step is exothermic (-15.88 kcal/mol) and the other two are highly endothermic (28.05 and 28.35 kcal/mol for the 2nd and 3rd abstraction respectively), make the overall hydrogen abstraction process highly endothermic (15.12 kcal/mol). The activation barrier has the highest value for the 2nd hydrogen abstraction step (NH_2*ad → NH*ad + H*ad), 41.2 kcal/mol (172.21 kJ/mol), and this is the rate limiting step for NH_3 dissociation over Mo_3N_2 cluster. Offermans *et al.* [38] also reported the 2nd hydrogen abstraction as the rate limiting step for Pt (111) surface and also found the same rate limiting step was reported by Duan *et al.* [36] for Ni (110) and by Mhadeshwar *et al.* [39] over Ru (0001) plane. Lanzania [37] reported the 1st hydrogen abstraction as the rate limiting step for NH_3 dissociation on nanosized iron cluster and Duan *et al*. [36] reported the 3rd hydrogen abstraction step as the rate limiting step. Mo_3N_2 cluster resembles Pt (111), Ru (0001) and Ni (111) plane regarding the rate-limiting step.

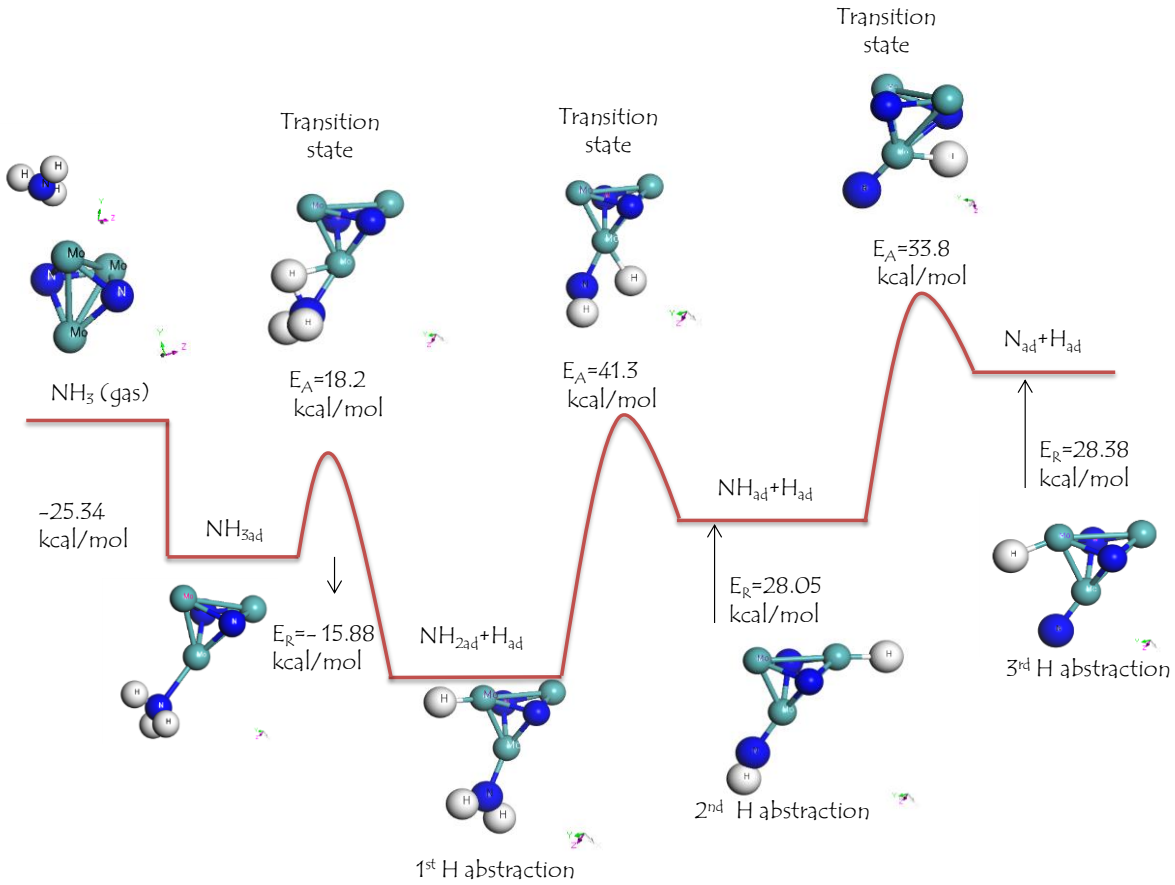

Fig. 4. Potential energy surface of ammonia dissociation over Mo3N2 cluster.

Table 2. Activation and reaction energies of hydrogen abstraction step for ammonia dissociation

Elementary reaction	Mo_3N_2 cluster		Pt(111) [38]		Ni(110) [35]		Fe cluster [37]		Co(111) [36]	
	Activation energy (ΔE_A) [kcal/mol]	Reaction energy (ΔE_R) [kcal/mol]	Activation energy (ΔE_A) [kcal/mol]	Reaction energy (ΔE_R) [kcal/mol]	Activation energy (ΔE_A) [kcal/mol]	Reaction energy (ΔE_R) [kcal/mol]	Activation energy (ΔE_A) [kcal/mol]	Reaction energy (ΔE_R) [kcal/mol]	Activation energy (ΔE_A) [kcal/mol]	Reaction energy (ΔE_R) [kcal/mol]
$NH_3^* \rightarrow NH_2^* + H^*$	18.2	-16.47	26.77	16.25	22.14	-5.76	34.13	-2.77	23.29	-3.23
$NH_2^* \rightarrow NH^* + H^*$	41.2	28.08	36.09	2.15	37.59	12.45	20.76	8.53	4.84	-10.15
$NH^* \rightarrow N^* + H^*$	33.8	28.38	34.42	18.88	20.52	6.68	7.84	-8.76	24.44	2.31
$N_2^* \rightarrow N^* + N^*$	35.19	22.44	x	x	38.74	0.59	x	x	42.89	14.30

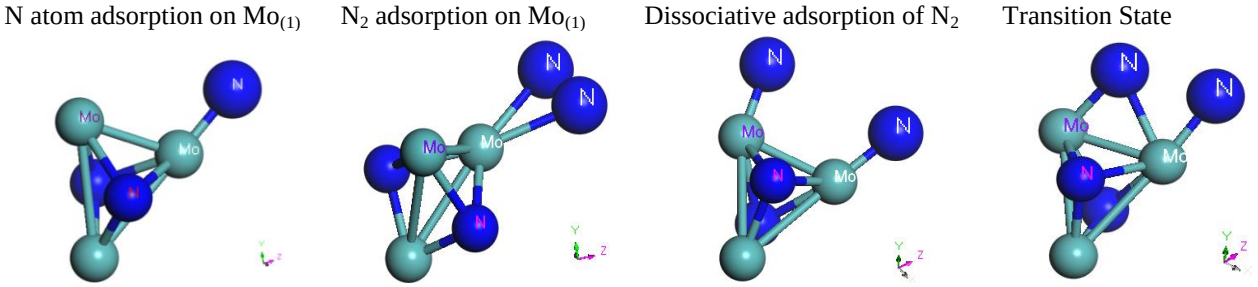

Fig, 5. Nitrogen adsorption and dissociation over Mo_3N_2 cluster.

NITROGEN ADSORPTION AND DISSOCIATION

Fig. 5 depicts the adsorption and dissociation of the nitrogen molecule. Atomic adsorption of the N atom on the $Mo_{(1)}$ atom of the cluster is −106.35 kcal/mol and when two N atoms adsorb on two different Mo atoms, $Mo_{(1)}$ and $Mo_{(2)}$, the adsorption energy is −103.73 kcal/mol, showing a small decrease due to interaction effects. The N_2 molecule adsorbed on the $Mo_{(1)}$ atom making a bond with two N atoms has an adsorption energy of −19.75 kcal/mol. The molecular nitrogen dissociation energy has an activation barrier of 35.19 kcal/mol and an endothermic reaction energy of 49 kcal/mol. The dissociation barrier of the N_2 molecule is 38.78 kcal/mol on Ni (110) surface [35], 43.82 kcal/mol on terraces of Ru (0001) surface [40], and 9.42 kcal/mol on steps of Ru(0001) [40] and 9.42 kcal/mol on V(110) surface [41]. Nitrogen dissociation is much more difficult on the Mo_3N_2 cluster compared to the other promising catalyst surfaces, which suggests that the ammonia decomposition follows the Tamaru mechanism over the Mo_3N_2 cluster, where ammonia activation and nitrogen desorption are rate limiting, similar to VN catalysts reported by Oyama *et al.* [42].

CONCLUSIONS

A DFT study was employed to determine the adsorption energy of NH_x (x = 1–3) and the transition state and the activation barrier of NH_3 dehydrogenation and N_2 dissociation over the Mo_3N_2 cluster. The results of calculations have shown that On-top adsorption configuration was the preferred adsorption arrangement for NH_x species over an Mo atom. The rate-limiting step for NH_3 decomposition is the second hydrogen abstraction step according to the following surface elementary reaction (NH_2*ad → NH*ad + H*ad) having an activation energy of 41.2 kcal/mol with an endothermic heat of reaction of 28.05 kcal/mol. Nitrogen dissociation has a barrier of 35.19 kcal/mol on the Mo_3N_2, which is much higher than on Ru and V catalysts.

Acknowledgment: *This work was supported by Chemical and Materials Engineering Department at King Abdulaziz University, Jeddah, Saudi Arabia.*

REFERENCES

1. B. L. Yi, Fuel Cells – Principle, Technology and Application, Chemical Industrial Publisher, Beijing, 2003.
2. A. S. Chellappal, C. M. Fischer, W. J. Thomson, *App. Catal. A*, **227**, 231 (2002).
3. L. F. Brown, *Int. J. Hydrog. Energy*, **26**, 381 (2001).
4. C. Zamfirescu, I. Dincer, *Fuel Proc. Tech*., **90**, 729 (2009).
5. S. F. Yin, B. Q. Xu, C. F. Ng, C. T. Au, *App. Catal. B: Environ.*, **52**, 287 (2004).
6. S. F. Yin, B. Q. Xu, X. P. Zhou, C. T. Au, *Appl. Catal. A*, **277**, 1 (2004).
7. J. Zhang, M. Comotti, F. Schuth, R. Schlogl, D. S. Su, *Chem. Commun.*, **17**, 1916 (2007).
8. R. Pelka, I. Moszynska, W. Arabczyk, *Catal. Lett.*, **128**, 72 (2009).
9. Y. Liu, H. Wang, J. F. Li, Y. Lu, Q. S. Xue, J. C. Chen, *AIChE*, **53**, 1845 (2007).
10. Y. Lu, H. Wang, Y. Liu, Q. S. Xue, J. C. Chen, M. Y. He, *Lab Chip*., **7**, 133 (2007).
11. X. K. Li, W. J. Ji, J. Zhao, S. J. Wang, C. T. Au, *J. Catal.*, **236**, 181 (2005).
12. T. V. Choudhary, D. C. Svammonia, D. W. Goodman, *Catal. Lett*., **72**, 197 (2001).
13. M. E. E. Abashar, Y. S. Al-Sughair, I. S. Al-Mutaz, *Appl. Catal. A*., **236**, 35 (2002).
14. A. Hellman, K. Honkala, I. N. Remediakis, D. A. Logammonia, A. Carlsson, S. Dahl, H. Christensen, J. K. Norskov, *Surf. Sci.*, **603**, 1731 (2009).
15. S. Dahl, D. A. Logammonia, R. C. Egeberg, J. H. Larsen, I. Chorkendorff, E. Tornqvist, J. K. Norskov, *Phys. Rev. Lett.*, **83**, 1814 (1999).
16. S. Dahl, E. Tornqvist, I. Chorkendorff, *J. Catal.*, **192**, 381 (2000).
17. P. F. Ng, L. Li, S. B. Wang, Z. H. Zhu, G. Q. Lu, Z. F. Yan, *Environ. Sci. Technol.*, **41**, 3758 (2007).
18. A. Klerke, S. K. Klitgaard, R. Fehrmann, *Catal. Lett.*, **130**, 541 (2009).
19. S. R. Deshmukh, A. B. Mhadeshwar, D. G. Vlachos, *Ind. Eng. Chem. Res.*, **43**, 2986 (2004).
20. A. M. Karim, V. Prash, G. Mpourmpakis, W. W. Lonergan, A. I. Frenkel, J. G. Chen, D. G. Vlachos, *J. Am. Chem. Soc.*, **131**, 12230 (2009).
21. W. Q. Zheng, J. Zhang, H. Y. Xu, W. Z. Li, *Catal. Lett.*, **119**, 311 (2007).
22. C. W. Seabury, T. N. Rhodin, R. J. Purtell, R. P. Merrill, *Surf. Sci.*, **93**, 117 (1980).
23. C. Egawa, T. Nishida, S. Naito, K. Tamaru, *J. Chem. Soc. Faraday Trans. I*, **80**, 1595 (1984).
24. F. Frechard, R .A. van Santen, A. Siokou, J. W. Niemantsverdriet, J. Hafner, *J. Chem. Phys.*, **111**, 8124 (1999).
25. S. Stolbov, T. S. Rahman, *J. Chem. Phys.*, **123**, 204716 (2005).
26. W. P. Krekelberg, J. Greeley, M. Mavrikakis, *J. Phys. Chem. B*, **108**, 987 (2004).
27. X. Z. Xiao, Y. L. Cao, Y. Y Cai, *Surf. Sci.*, **605**, 802 (2012).
28. W. Tsai, W. H. Weinberg, *J. Phys. Chem.*, **91**, 5302 (1987).
29. W. Kohn, L. J. Sham, *Phys. Rev.*, **140**, A1133 (1965).
30. J. P. Perdew, J. A. Chevary, S. H. Vosko, K. A. Jackson, M. R. Pederson, D. J. Singh, C. Fiolhais, *Phys. Rev. B*, **46**, 6671 (1992).
31. A. D. Becke, *J. Chem. Phys*., **88**, 2547 (1988).

32. J. P. Perdew, Y. Wang, *Phys. Rev. B*, **45**, 13244 (1992).
33. T. A. Halgren, W. N. Lipscomb, *Chem. Phys. Lett.*, **49**, 225 (1977).
34. S. Bell, J. S. Crighton, *J. Chem. Phys.*, **80**, 2464 (1983).
35. X. Duan, G. Qian, C. Fan, Y. Zhu, X. Zhou, D. Chen, W. Yuan, *Surf. Sci.*, **606**, 549 (2012).
36. G. Lanzania, K. Laasonen, *Int. J. Hydrog. Energy*, **35**, 6571 (2010).
37. X. Duan, J. Ji, G. Qian, C. Fan, Y. Zhu, X. Zhou, D. Chen, W. Yuan, *J. Mol. Catal. A: Chem*., **357**, 81 (2012).
38. W. K. Offermans, A. P. J. Jansen, R. A. van Santen, G. Novell-Leruth, J. M. Ricart, J. Pérez-Ramírez, *J. Phys. Chem. C*, **111**, 17551 (2007).
39. A. B. Mhadeshwar, J. R. Kitchin, M. A. Barteau, D. G. Vlachos, *Catal. Lett.*, **96**, 13 (2004).
40. A. Logadottir, J. K. Norskov, *J. Catal.*, **220**, 273 (2003).
41. P. Rochana, K. Lee, J. Wilcox, *J. Phys. Chem. C*, **118**, 4238 (2014).
42. J. J. Spivey, K. M. Dooley, *Catalysis*, **19**, 84 (2006).

ИЗСЛЕДВАНЕ С ТФП НА ДИСОЦИАЦИЯТА НА АМОНЯК ВЪРХУ КЛЪСТЕР Mo_3N_2

Ш. Ф. Заман

Chemical and Materials Engineering Department, Faculty of Engineering, King Abdulaziz University, P.O. Box 80204, Jeddah 21589, Saudi Arabia

Постъпила на: 5 февруари 2018 г.; Преработена на: 4 март 2018 г.

(Резюме)

С метода на ТФП е изследван механизма на процеса на разлагане на амоняк върху Mo_3N_2 клъстер. Моделирани са елементарните стадии на повърхностните реакции след адсорбция на NH_x (x = 0–3) частици "on-top" върху Mo атоми. Тази конфигурация на повърхностните активни комплекси е енергитично най-изгодна. Скорост определящият стадий на разлагането на амоняка (NH_2*ad → NH*ad + H*ad) е с активираща енергия от 41.2 kcal/mol и ендотермична топлина на стадия 28.1 kcal/mol. Енергията на дисоцияция на адсорбирания N_2 е 35.19 kcal/mol и е значително по-висока от тази на N_2 адсорбиран на Ru(0001).